Since January 2020 Elsevier has created a COVID-19 resource centre with free information in English and Mandarin on the novel coronavirus COVID-19. The COVID-19 resource centre is hosted on Elsevier Connect, the company's public news and information website.

Computers in Biology and Medicine 146 (2022) 105552

Contents lists available at ScienceDirect

Computers in Biology and Medicine

journal homepage: www.elsevier.com/locate/compbiomed

Curcumin inhibits spike protein of new SARS-CoV-2 variant of concern (VOC) Omicron, an *in silico* study

Anish Nag [a,*], Ritesh Banerjee [b], Subhabrata Paul [c], Rita Kundu [d]

[a] Department of Life Sciences, CHRIST (Deemed to be University), Bangalore, Karnataka, 560029, India
[b] School of Biological and Environmental Sciences, Shoolini University, Solan, Himachal Pradesh, 173229, India
[c] School of Biotechnology, Presidency University, Canal Bank Rd, DG Block, Action Area 1D, New Town, West Bengal, 700156, India
[d] Department of Botany, University of Calcutta, Kolkata, West Bengal, 700019, India

ARTICLE INFO

Keywords:
COVID-19
Coronavirus
Spike-RBD
Omicron
In silico study

ABSTRACT

Background: Omicron (B.1.1.529), a variant of SARS-CoV-2 is currently spreading globally as a dominant strain. Due to multiple mutations at its Spike protein, including 15 amino acid substitutions at the receptor binding domain (RBD), Omicron is a variant of concern (VOC) and capable of escaping vaccine generated immunity. So far, no specific treatment regime is suggested for this VOC.

Methods: The three-dimensional structure of the Spike RBD domain of Omicron variant was constructed by incorporating 15 amino acid substitutions to the Native Spike (S) structure and structural changes were compared that of the Native S. Seven phytochemicals namely Allicin, Capsaicin, Cinnamaldehyde, Curcumin, Gingerol, Piperine, and Zingeberene were docked with Omicron S protein and Omicron S-hACE2 complex. Further, molecular dynamic simulation was performed between Crcumin and Omicron S protein to evaluate the structural stability of the complex in the physiological environment and compared with that of the control drug Chloroquine.

Results: Curcumin, among seven phytochemicals, was found to have the most substantial inhibitory potential with Omicron S protein. Further, it was found that curcumin could disrupt the Omicron S-hACE2 complex. The molecular dynamic simulation demonstrated that Curcumin could form a stable structure with Omicron S in the physiological environment.

Conclusion: To conclude, Curcumin can be considered as a potential therapeutic agent against the highly infectious Omicron variant of SARS-CoV-2.

1. Introduction

After emerging in 2019 at Wuhan, China, the modern-day global pandemic COVID-19 is still a major health threat with more than 300 million cases and 5.5 million deaths to date [1]. With the error-prone RNA polymerase, we have witnessed the emergence of several SARS-CoV-2 variants in due time of viral evolution. WHO classified these variants into three categories; VOIs: variants of interests, VUMs: variants under monitoring, and the most important VOCs: variants of concern [2]. The most recent VOC, Omicron (B.1.1.529) has been designated by WHO as the fifth VOC after Alpha, Beta, Gamma and Delta variants. With the emergence in November 2021 in South Africa, this variant spread worldwide at an alarming rate and was found to be the most prevalent form among the VOCs including India [3]. Similar to other VOCs, several spike mutations had been observed in Omicron that enabled varying degrees of escape from neutralizing antibodies and confer increased transmissibility [4–6]. More than 60 different mutations accumulated in the Omicron variant (CoVariants GISAID), made it the variant with the largest number of mutations. These mutations, especially the ones in the receptor binding domain (RBD) of the viral Spike are responsible for the immune escape, disease progression and enhanced transmission of the virus [7]. Noteworthy mutations at positions N440K, N501Y are associated with greater infectivity and transmissibility [8,9]. Recent evidences suggested that some of the most used COVID-19 vaccines provide little or no protection against the infection caused by the Omicron variant [10]. Thus, the Omicron variant might undermine global efforts to control the COVID-19 pandemic by emerging as a potential threat to public health. In our previous study

* Corresponding author.
E-mail address: anish.nag@christuniversity.in (A. Nag).

https://doi.org/10.1016/j.compbiomed.2022.105552
Received 12 February 2022; Received in revised form 17 April 2022; Accepted 20 April 2022
Available online 27 April 2022

[11], we have predicted the accumulation of 12 mutations in a hypothetical spike protein which was expected to have greater binding affinity to the human Angiotensin Converting Enzyme 2 (hACE2). Four substitution positions at 477, 478, 484 and, 501 are the common mutations that are shared between our previously predicted and the newly emerged Omicron Spike proteins. The search for potent phyto-molecules against SARS-CoV-2 is in progress to directly target the viral proteins.

Identifying phytochemicals as effective drug candidates requires enormous time and capital investment. In this regard, screening drug molecules through target specific advanced computational approaches such as molecular docking, molecular dynamic simulation are in continuous demand that saves both time and resources [12,13]. Literature indicated that, a comprehensive approach in drug discovery can be achieved by combining *multiple in silico* databases and tools such Therapeutic Target Database, Drug Bank etc [14,15].

Recently, molecular dynamics (MD) simulation and binding free energy calculation by Molecular Mechanics-Poisson–Boltzmann Solvent-Accessible surface area (MM-PBSA) method coupled with molecular docking technique further facilitated advancement in drug discovery with high precision and accuracy [16–19].

Several phytochemicals were being tested by *in silico* methods that can act as potent drug components in treating SARS-CoV-2 infection [20] and proteins such as main protease and Spike protein were utilized as the drug targets [21,22]. However, Receptor Binding Domain (RBD) of the Spike protein is one of the most common targets for the inhibition of cellular entry of SARS-CoV-2 [11,23]. Nevertheless, to the best of our knowledge, no reports are available to date regarding therapeutic phytochemicals specific to viral proteins of VOC Omicron. In our previous study, among seven compounds screened, two phytochemicals, piperine and curcumin, were found to have strong binding affinity for our predicted mutated Spike and expected to reduce the stability of Spike-hACE2 complex. Those observations led us to this present study, which aims to screen those seven phytochemicals and identify potential therapeutic candidate against the Omicron variant.

2. Experimental

2.1. Sequence retrieval of Omicron Spike (S), and sequence alignment with native S

The primary sequence of the Native Spike (S) protein (start position 333), was obtained from GISAID [24]. Further, 15 mutations were introduced into Native S by using PyMol 2.5 software and Omicron S was formed. The multiple sequence alignment of Native and Omicron S protein sequences were performed by Clustal Omega web server (https://www.ebi.ac.uk/Tools/msa/clustalo/). The three dimensional structures of Native S (PDB id 6M0J, Chain E, X-Ray Diffraction, Resolution 2.45 Å) and hACE2 (PDB id 6M0J, Chain A) were optimized as per our previous study [11].

2.2. Structural comparison with native S

The effect of mutations on the Omicron variant of the Spike (S) protein was initially examined and visualized by UCSF Chimera software. This software was used to evaluate the conformation changes of Omicron S and compared with that of the Native S. Further, the flexibility of Native and Omicron S proteins were performed by CABS-flex 2.0 (http://biocomp.chem.uw.edu.pl/CABSflex2) software. The effect on protein stability due to residual mutations of Omicron S protein was evaluated by Site Directed Mutator 2 (SDM2) server (http://marid.bioc.cam.ac.uk/sdm2). SDM2 uses knowledge based approach to predict effect of individual amino acid mutations in conformationally constrained environment-dependent amino acid substitutions. The results were expressed in a tabular format for both wild and mutant types with the parameters namely Occluded Surface Packing value (OSP), Residual depth, Residue relative to solvent accessibility (RSA %), and Predicted stability change (ΔΔG). While, Occluded surface of a given residue represents the 2.8 Å surrounding molecular surface of non-bonded atoms, OSP of a given residue is the function of Occluded surface area and average normal unit distance between non bonded atom molecular surface & neighboring van Der Waals surface. Residual depth of a given residue represents average distance between all atom depths and the nearest water molecule surface. Solvent accessibility of any residue is expressed by the term RSA (%). Finally, ΔΔG is the free energy difference between wild type and mutant type residues [25].

2.3. Protein-protein docking

Omicron S and hACE2 docking was performed by using ClusPro protein-protein docking web-server (https://cluspro.bu.edu/login.php). Cluspro rotates the ligand in 70000 combinations and selects the best 1000 low energy structures from those. The best result is suggested based on the nearest 9 Å position of the ligand [26]. For the prediction of binding energy and molecular interaction sites of the complex, PRODIGY (https://wenmr.science.uu.nl/prodigy/) was used.

2.4. Phytochemical-protein molecular docking

Three dimensional structures of the seven phytochemicals namely allicin (PubChem id 65036), capsaicin (PubChem id 1548943), Cinnamaldehyde (PubChem id 637511), Curcumin (PubChem id 969516), Gingerol (PubChem id 44279), Piperine (PubChem id 638024), Zingeberene (PubChem id 92776) and two control drugs namely Chloroquine (PubChem id 2719) and GR 127935 hydrochloride (PubChem id 107780) were docked with Omicron S protein and Omicron S-hACE2 complex by using Dockthor docking server (https://dockthor.lncc.br/v2/). Chloroquine is a common inhibitory molecule against Spike (S) protein in *in silico* studies [11,27], while GR 127935 hydrochloride is a control drug against hACE2 [11,28] in literature. Optimization was performed as per the procedure described by Nag et al. [11]. Dockthor utilizes inhouse flexible docking tools, namely MMFF Ligand and PdbThorBox. It is a powerful docking software, that applies MMFF94S53 force field for the protein inputs [29]. The grid parameters were selected based on the interaction site between Spike protein and hACE2 and were set as x/y/z = - 39/36/8 & size x = 24/29/20 and x/y/z = −42.25/12.621/-43.746 & size x/y/z = 34/20/21 for Omicron S and Omicron S-hACE2 complex respectively. The phytochemical docking results (binding energy kcal/mol) were compared with that of the spike (Chloroquine) and hACE2 (GR 127935 hydrochloride) controls. The interacting amino acids and bonds of the ligand-protein complexes were analyzed by BIOVIA Discovery Studio Visualizer (Dassault Systems) software.

2.5. Docking validation by molecular dynamic (MD) simulation

The MD simulation of curcumin and Omicron S protein was performed by GROMACS-2019.2 [30] based bio-molecular package of Simlab, the University of Arkansas for Medical Sciences (UAMS), Little Rock, USA and as per the procedure described in our previous paper [11]. Briefly, set up parameters were SPC water, 0.15 M counter ions (Na+/Cl-), NVT/NPT ensemble temperature 300 K & atmospheric pressure (1 bar) and the ligand topology file was generated by PRODRG software [31]. The result was expressed based on the selected output parameters, namely Root Mean Square Deviation (RMSD), the Radius of Gyration (Rg), Root Mean Square Fluctuation (RMSF), Solvent Accessible Surface Area (SASA), and H bonds. The simulation length was set as 100 ns.

2.6. Free energy analysis by MM-PBSA calculation

The free energies of Chloroquine-Omicron S and Curcumin-Omicron S complexes (ΔG_Vander Waal, ΔG_Electrostatic, ΔG_Polar, ΔG_Non-

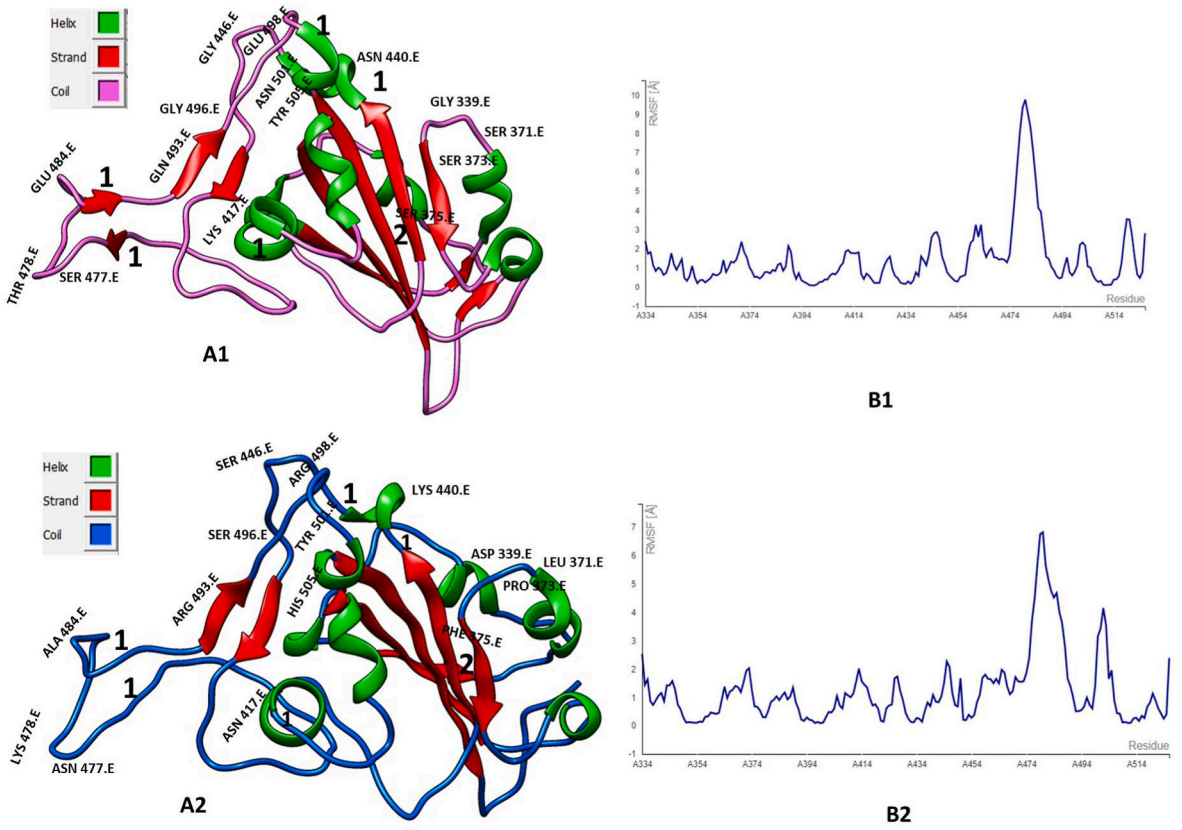

Fig. 1. Comparative evaluation of structural changes due to mutations in Omicron spike protein
A: 3D structures of proteins as rendered by UCSF Chimera (**A1**: Native spike protein and **A2**: Omicron Spike protein; **1**: Change of structure from Helix to Coil, **2**: Wavy strand); **B:** Flexibility analysis of the amino acid residues as determined by CABS-Flex 2.0 (**B1**: Native spike protein and **B2**: Omicron Spike protein).

Polar, ΔG_Binding and residual contribution energy) were estimated by Molecular Mechanics-Poisson–Boltzmann Solvent-Accessible surface area (MM-PBSA) method using g-mmbsa package [32].

Following equation was used for calculating ΔG_Binding (KJ mol^{-1}):

$$\Delta G\_Binding = G\_Comp - (G\_Prot + G\_Lig)$$

ΔG_Comp represents the energy of protein-ligand complexes, G_Prot and G_Lig are individual energy of protein and ligand respectively. The MMPBSA calculation was performed for 5 ns trajectory.

2.7. Structural changes in the Omicron S protein after binding of curcumin

The effect of Curcumin binding on the target protein Omicron S was evaluated by PyMol 2.5 software. A few amino acid residues were randomly flagged at different positions of the Omicron S and Omicron S + Curcumin proteins, and residual distances were measured & compared by the 'Measurement Wizard' function.

Table 1
Change in Omicron S protein stability upon mutations.

Mutation	WT_RSA (%)	WT_Depth (Å)	MT_OSP	MT_RSA (%)	MT_Depth (Å)	MT_OSP	Predicted ΔΔG	Outcome
GLY**339**ASP	89.0	3.4	0.28	100.1	3.3	0.16	0.17	**Increased stability**
SER**371**LEU	46.3	3.3	0.31	61.6	3.5	0.24	0.60	**Increased stability**
SER**373**PRO	71.9	3.5	0.19	66.9	3.4	0.17	−0.62	Reduced stability
SER**375**PHE	65.6	3.6	0.2	73.8	3.4	0.15	0.52	**Increased stability**
LYS**417**ASN	47.6	3.6	0.3	49.0	3.9	0.3	−1.34	Reduced stability
ASN**440**LYS	93.6	3.3	0.15	103.8	3.1	0.07	0.87	**Increased stability**
GLY**446**SER	115.4	3.4	0.17	103.5	3.2	0.12	−4.11	Reduced stability
SER**477**ASN	101.6	3.1	0.14	118.8	3.1	0.1	0.22	**Increased stability**
THR**478**LYS	84.2	3.4	0.17	72.6	3.3	0.15	0.01	**Increased stability**
GLU**484**ALA	58.3	3.5	0.22	60.7	3.1	0.17	0.42	**Increased stability**
GLN**493**ARG	56.2	3.6	0.28	65.9	3.5	0.22	−0.02	Reduced stability
GLY**496**SER	21	3.9	0.34	27.1	3.7	0.38	−0.58	Reduced stability
GLN**498**ARG	40.1	3.6	0.39	42.4	3.6	0.4	0.09	**Increased stability**
ASN**501**TYR	27.9	4.1	0.36	30.3	4.1	0.39	0.69	**Increased stability**
TYR**505**HIS	65.4	3.5	0.29	60.0	3.5	0.31	−0.06	Reduced stability

WT: Wild Type and MT: Mutant Type**, RSA (%)**: Residue relative to solvent accessibility; **OSP:** Occluded Surface Packing value; **ΔΔG**: Predicted stability change.

3. Results and discussion

3.1. Sequence retrieval of Omicron Spike (S), and sequence alignment with native S

The sequence of Omicron S protein and its alignment with the Native S (Fig. S1) are shown in the supplementary file.

3.2. Structural comparison of Omicron and native S

Omicron S protein accommodates 15 mutations at its receptor binding domain (RBD). These point mutations significantly affected the structural conformation when compared with the Native S protein. We observed multiple helix-coil transitions in the Omicron S protein at multiple sites as represented in Fig. 1 A1 and A2. Structural deviation in the Omicron S protein could be attributed to some of these mutated amino acid residues such as ASN477, LYS478, ALA484, ASN417, ARG419, TYR501 and PHE375. In our earlier study [11], we prepared a hypothetical RBD domain of S protein and compared it with that of the original (Native) structure. The hypothetical S protein shared four common mutations as of the Omicorn variant, and we also observed similar structural modifications. Residual flexibility is an important intrinsic property of protein, which allows a broad range of interaction with multiple targets [33]. When Omicron S was compared with the Native S, we observed a marginal increase in the residual flexibility in the regions of mutated residues as presented in Fig. 1 B1 and B2. Furthermore, Table 1 represents the effect of Spike mutations on the stability of the protein with respect to the wild type variant. Among the 15 mutations in the Omicron S, we observed nine residues (ASP339, LEU371, PHE375, LYS440, ASN477, LYS478, ALA484, ARG498, and TYR501) directly contributed to increase the stability of the protein, as shown by various parameters such as RSA%, Residual depth, OSP and free energy difference (ΔΔG). While free energy change represented the effect of stability of protein, earlier study showed that ΔΔG could be directly correlated with other structural parameters as mentioned above [34,35]. In agreement with our findings, previous literatures have reported that mutated amino acids such as ASP339, LEU371, PRO373 and PHE375 are unique residues which could significantly contribute towards the higher binding capacity of Spike protein to the hACE2 as well as invasion of antibodies [36–39]. Overall, these findings indicated that substitutions in the composition of amino acids of the Omicron variant might favour enhanced and improved binding potential to hACE2, which could result in higher transmissibility of the SARS-CoV-2 virus.

3.3. hACE2-Omicron spike interaction

First reported in South Africa, the Omicron variant of SARS-CoV-2 was reported to have higher transmissibility (three to six times) than the other prevailing stains, including Delta [40]. To investigate whether this transmissibility can be translated towards the higher ligand-protein interaction, we compared the binding energies of Native and Omicron S to the hACE2. Prodigy evaluation revealed the binding energy between hACE2 and Omicron S protein as −13.7 kcal mol^{-1}. In our previous study, we reported the binding energies of the Native and hypothetical mutated S proteins as −12.6 and −13.2 kcal mol^{-1}, respectively [11]. While the binding energies were comparable for our predicted S and Omicron S proteins, Native S showed weak binding potential with the hACE2 in comparison. Therefore, similar to our hypothetical S protein, Omicron S, which shared four common mutations with the former, had strong binding potential with the hACE2.

3.4. Phytochemical-protein (Omicron S/Omicron S+ hACE2) interaction

Docking results of seven phytochemicals (Allicin, Capsaicin, Cinnamaldehyde, Curcumin, Gingerol, Piperine, and Zingeberene) with target proteins (Omicron S/Omicron S+ hACE2) were analyzed along specific controls for S and hACE2, namely chloroquine and GR 127935 hydrochloride respectively (Table 2). The result showed that the phytochemical curcumin could strongly bind with both Omicron S and Omicron S + hACE2 complex (−8.473 and 8.316 kcal mol^{-1}, respectively) compared with the respective control drugs (−7.698 and −5.479 kcal mol^{-1}). Curcumin had been consistently reported as the therapeutic agent against SARS-CoV-2 through blocking Spike protein. We earlier reported curcumin as the potential agent against SARS-CoV-2 S proteins, both Native and mutated [11]. Jena et al. [41] showed that this phytochemical could inhibit S protein and disrupt the S-hACE2 complex. Marin-Palma et al. [42], further demonstrated that curcumin could inhibit SARS-CoV-2 *in vitro* in Vero E6 cell line. In the current work, curcumin was found to bind with multiple mutated amino acid residues (SER114 [446], ARG161 [493], SER164 [496], and HIS173 [505]) of Omicron S protein along with other residues (Table 3). However, control drug Chloroquine could only bind with the mutated amino acid ARG161. This was indicative that Curcumin might have higher affinity towards Omicron S, than Chloroquine. Nevertheless, Chloroquine and the phytochemical Curcumin shared the same pocket of Omicron S consisting of common amino acids TYR117 [449], ARG161 [493], and SER162 [494]. In our previous work, we evaluated the interaction sites

Table 2
Binding affinities (Kcal mol^{-1}) between compounds and proteins (Omicron S and Omicron S + hACE2).

PubChem CID	Compounds	Binding affinities (Kcal mol^{-1})	
		Omicron Spike	Omicron Spike + hACE2
2719	Chloroquine[a]	−7.698	−7.460
107780	GR 127935 hydrochloride**	NA	−5.479
65036	Allicin	−7.214	−6.880
1548943	Capsaicin	−8.072	−7.654
637511	Cinnamaldehyde	−6.737	−6.755
969516	Curcumin	**−8.473**	**−8.316**
442793	Gingerol	−7.896	−7.951
638024	Piperine	−7.439	−8.433
92776	Zingeberene	−7.868	−7.738

[a] Spike inhibitor as a control; ** hACE2 inhibitor as a control; **Bold** = highest binding affinity (Kcal mol^{-1}).

Table 3
Interacting amino acids between Controls, Curcumin and proteins (Omicron S and Omicron S + hACE2 complex).

Compound + Proteins	Interacting bonds			
	Pi Bond	Carbon H	Attractive Charge	Conventional H
Chloroquine + Omicron Spike	LEU160E, **ARG161E**, SER162E	LEU160E, **ARG161E**, SER162E	… … … … ….	TYR117E
Chloroquine + Omicron Spike + hACE2	PHE124E	LEU123E	LYS156A, GLU74E	–
GR 127935 hydrochloride + Omicron Spike + hACE2	VAL18E, ILE70E, TYR157E, GLU148A	PRO474A	GLU74E, ASP476A	LYS156A
Curcumin + Omicron Spike	TYR117E, ARG71E	**SER114E**, **ARG161E**,	… … … …. .	TRY121E, SER162E, **SER164E**, **HIS173E**
Curcumin + Omicron Spike + hACE2	GLU74E, LEU123E, **HIS173E** PRO160A, TYR479A	LYS156A, PRO474A, ASP476A	… … … … … …	TYR121E

Bold: mutated amino acid, Chain E: Omicron spike protein, Chain A: hACE2 protein.

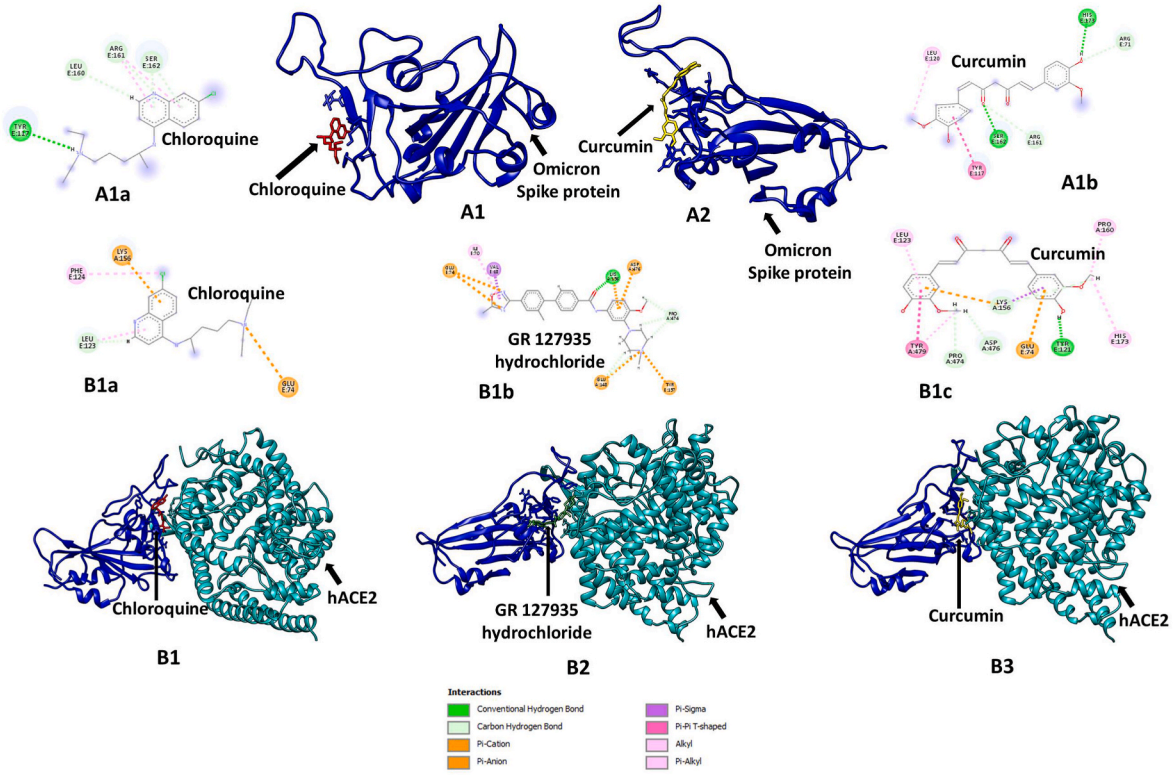

Fig. 2. Interaction of selected ligands with Omicron S protein and Omicron S-hACE2 complex; A1 and A2: 3D representations of Chloroquine and Curcumin interaction with Omicron S proteins; **B1, B2 and B3**: 3D representations of Chloroquine, Curcumin, and GR 127935 hydrochloride interactions with Omicron S-hACE2 complex; **A1a and A1b:** 2D representations of amino acid interactions of Chloroquine-Omicron S and Curcumin-Omicron S; **B1a, B1b and B1c:** 2D representation of amino acid interactions of Chloroquine-Omicron S-hACE2, GR 127935 hydrochloride- Omicron S-hACE2 and Curcumin-Omicron S- hACE2 complexes.

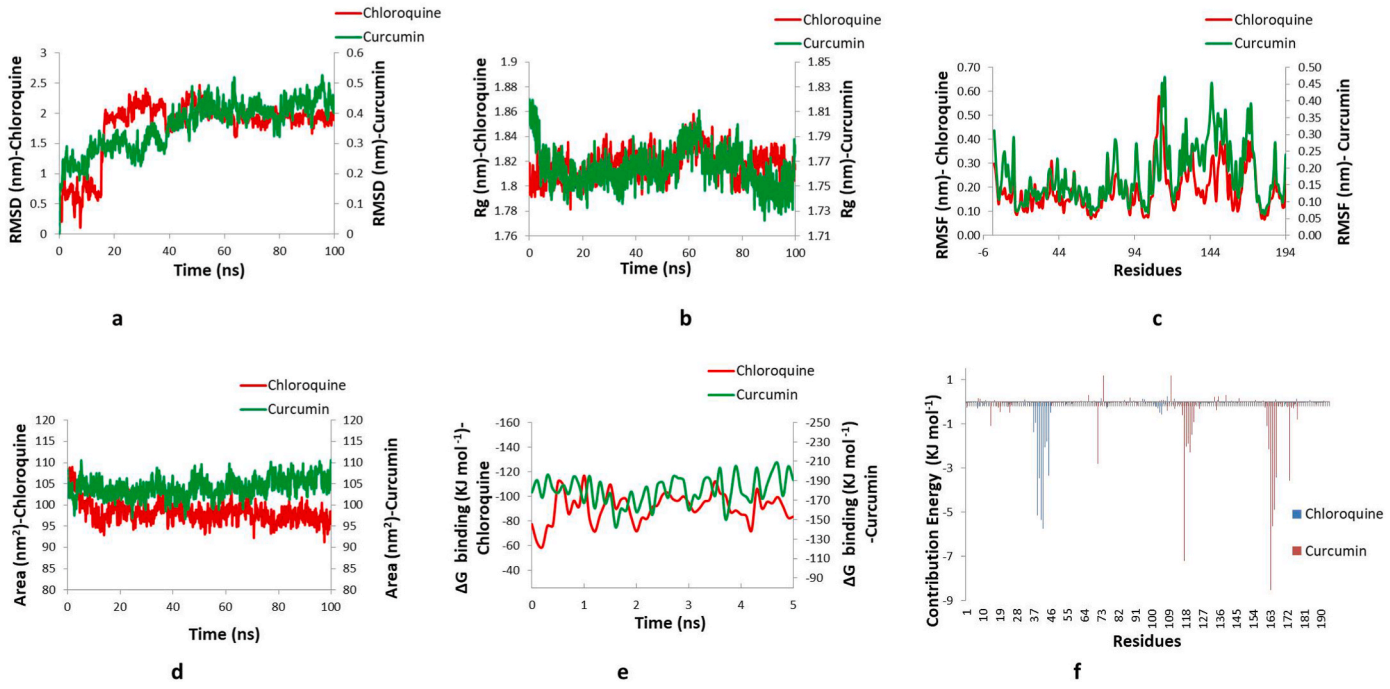

Fig. 3. MD simulation line plots of Curcumin and Omicron S protein; **(a)** Root Mean Square Deviation (RMSD), **(b)** Radius of gyration (Rg) line plots, **(c)** Root Mean Square Deviation (RMSF), **(d)** Solvent Accessible Surface Area (nm^2), (**e**) ΔG binding energy (KJ mol^{-1}), (**f**) Residual contribution energy (KJ mol^{-1}).

of Curcumin with the Native S protein and SER162 [494] was found as a common interacting residue with that of Omicron S [11]. Further, we observed multiple interaction points of curcumin to the hACE2 in the Omicron-S complex. These residues are major hACE2 and Omicron S interacting amino acids (Fig. 2). Unlike the ACE control GR 127935 hydrochloride, curcumin formed pi-bond with the mutated spike residue

Table 4
MM-PBSA calculations of binding free energy for Chloroquine and Curcumin-Omicron S complex.

Types of Binding Energy	Binding energy Chloroquine-Omicron S complex	Binding energy Curcumin-Omicron S complex
ΔG binding (KJ mol^{-1})	−90.89 ± 12.33	−180.04 ± 15.16
ΔG Non polar (KJ mol^{-1})	−8.84 ± 1.10	−16.16 ± 1.27
ΔG polar solvation (KJ mol^{-1})	24.57 ± 8.12	61.22 ± 7.26
ΔG Electrostatic (KJ mol^{-1})	−1.12 ± 1.11	−13.52 ± 4.26
ΔG Van der Waal (KJ mol^{-1})	−105.50 ± 14.24	−211.58 ± 16.35

HIS173 [505], revealing its stronger affinity towards mutated protein in the complex. Hence, it was evident that curcumin showed two-way interactions. If administered early, it could bind with the Omicron S RBD, blocking its interaction with hACE2. In case of late administration, curcumin could disrupt the structural stability of the Omicron S+ hACE2 complex by binding with the interacting site.

3.5. Molecular dynamic (MD) simulation of Curcumin and Omicron S

We further evaluated the structural dynamics and stability of the curcumin-Omicron S complex in the near-native biological environment by using MD simulation tool and compared with that of the Control (Chloroquine)-Omicron S complex. Collectively data processed from four parameters namely Root Mean Square Deviation (RMSD), Radius of gyration (Rg), Solvent Accessible Surface Area (SASA) and ligand-protein H bond formations showed a comparable binding profiles for both Chloroquine and Curcumin to the Omicron S target. RMSD represents the contact between protein residues and ligand. While, Chloroquine showed average RMSD of 1.8 nm, Curcumin had the mean RMSD of 0.35 nm. Low RMSD of Curcumin, essentially showed better fitting of the ligand to the cavity of the target protein. However, the RMSD profiles were comparable and both the compounds stabilized after 40 ns of simulation (Fig. 3a). Rg represented the compactness of the protein. We did not find any marked difference of Rg values between two complexes. For Curcumin, while Rg ranged from 1.7 to 1.85 nm, Chloroquine showed similar range of 1.75–1.85 nm (Fig. 3b). Therefore, ligand binding did not affect the compactness of the protein Omicron S for both the cases. Similar to the Rg values, residual fluctuations as revealed by RMSF values are comparable for both the complexes (Chloroquine 0.07 to 0.57 and Curcumin 0.06–0.47 nm). We observed marked fluctuations in the amino residue number zone of 150–170 of the target protein S, possibly due to binding and rotation of the ligands (Fig. 3c). Solvent accessible areas were comparable and stable throughout the simulation timeframe for both the complexes as seen in Fig. 3d. It was also found that minimum 1H bond was maintained throughout the Curcumin-Omicron S simulation, and the interaction was not robust for Chloroquine (Fig. S2). Overall, MD simulation revealed that Curcumin could form a stable structure with the Omicron S protein in the physiological environment and could possibly form stronger interaction than the control drug Chloroquine.

3.6. Free energy analysis by MM-PBSA calculation

Literature showed that, MM-PBSA method could effectively estimate the fee energy of binding of the docked complexes. Although it requires high computational cost, it can still provide near accurate result than the conventional molecular docking technique [43,44]. The results showed that when compared with the control drug Chloroquine (ΔG binding −90.89 ± 12.33 kJ mol^{-1}), Curcumin had a very high binding affinity (ΔG -180.04 ± 15.16 kJ mol^{-1}) towards the receptor protein Omicron S. Further, this observation was supported by higher contribution of other energy terms namely ΔG Non polar, ΔG Electrostatic and ΔG van der Waals as shown in Table 4. Low contribution of unfavorable polar solvation energy was also seen for both the compounds. Both the complexes showed stable free binding energy profiles throughout the simulation cycle (Fig. 3e). Overall Curcumin showed higher affinity towards Omicron S, than that of the control drug Chloroquine. Finally, it was found that ASP339 (7), LYS440 (108), SER446 (114), LYS478 (146), ARG493 (161), SER496 (164), ARG498 (166), TYR501 (169), and HIS505 (173) are the major mutated amino acid residues contributed towards toward the enhanced binding of Curcumin to the target protein Omicron S (Fig. 3f).

3.7. Structural changes in the Omicron S protein after binding of curcumin

To understand the structural changes of Omicron S protein, due to binding of the ligand Curcumin, post MD simulation Curcumin-Omicron S complex was selected. Measured distance values between randomly flagged amino acids of the respective proteins (Omicron S with and without Curcumin) revealed the conformation changes of the protein (Fig. 4). The results indicated that, there was potential decrease among the amino acid distances of Curcumin complex when compared to that of the unbound one. It could be hypothesized from the results that such changes might inhibit the complex to bind with hACE2, hence, preventing the entry of the SARS-CoV-2 pathogen inside the cell.

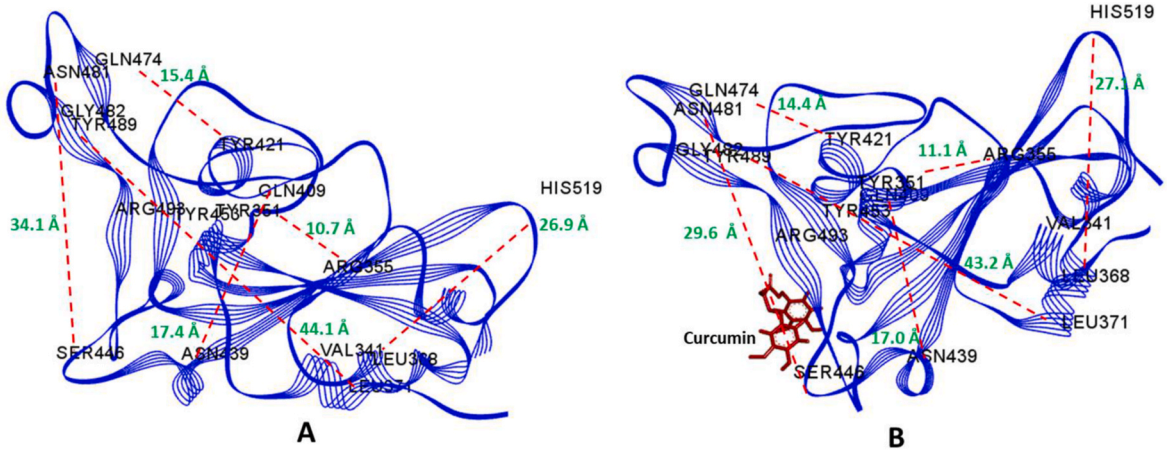

Fig. 4. Structural comparison with ligand free (A) and bound Omicron S, as determined by PyMol 2.0 software.

4. Conclusion

The present study reported curcumin as a potential therapeutic candidate against the SARS-CoV-2 Omicron variant among seven phytochemicals studied. It inhibited the mutated Spike protein of Omicron S through interaction with various amino acids, including the substituted ones such as SER446 (114), ARG493 (161), SER496 (164) and HIS505 (173). Further investigation suggested that Curcumin could destabilize the ACE2-S complex, as well. Molecular dynamic simulation and MM-PBSA study finally revealed that Curcumin formed a stable structure with Omicron S protein through H bond formation.

Author contributions

A.N. conceived, designed the study & performed the experimentations; Primary data analysis & manuscript draft preparation were done by S.P. Secondary data analysis was done by RB and proof reading & manuscript finalisation was done by R.K. All authors read and approved the final manuscript.

Declaration of competing interest

Authors declare that there is no conflict of interest.

Acknowledgements

Authors duly acknowledge Department of Life Sciences, CHRIST (Deemed to be University); Bangalore; School of Biotechnology, Presidency University, Kolkata, School of Biological and Environmental Sciences, Shoolini University, Solan, Himachal Pradesh and Department of Botany, University of Calcutta, Kolkata, West Bengal for providing institutional and administrative supports as and when required.

Appendix A. Supplementary data

Supplementary data to this article can be found online at https://doi.org/10.1016/j.compbiomed.2022.105552.

References

[1] WHO Coronavirus (COVID-19) Dashboard n.d. https://covid19.who.int (accessed January 27, 2022).
[2] X. He, W. Hong, X. Pan, G. Lu, X. Wei, SARS-CoV-2 Omicron variant: characteristics and prevention, MedComm 2 (2021) 838–845, https://doi.org/10.1002/mco2.110.
[3] INSACOG | Department of Biotechnology n.d. https://dbtindia.gov.in/insacog (accessed January 27, 2022).
[4] A.J. Greaney, T.N. Starr, J.D. Bloom, An antibody-escape calculator for mutations to the SARS-CoV-2 receptor-binding domain, bioRxiv (2021), https://doi.org/10.1101/2021.12.04.471236, 2021.12.04.471236.
[5] C. Tong, W. Shi, A. Zhang, Z. Shi, Tracking and controlling the spatiotemporal spread of SARS-CoV-2 Omicron variant in South Africa, Trav. Med. Infect. Dis. 46 (2022), 102252, https://doi.org/10.1016/j.tmaid.2021.102252.
[6] X. Zhang, S. Wu, B. Wu, Q. Yang, A. Chen, Y. Li, et al., SARS-CoV-2 Omicron strain exhibits potent capabilities for immune evasion and viral entrance, Signal Transduct. Targeted Ther. 6 (2021) 1–3, https://doi.org/10.1038/s41392-021-00852-5.
[7] CDC, CDC Works 24/7. Centers for Disease Control and Prevention. https://www.cdc.gov/index.htm, 2022. (Accessed 27 January 2022).
[8] B. Korber, W.M. Fischer, S. Gnanakaran, H. Yoon, J. Theiler, W. Abfalterer, et al., Tracking changes in SARS-CoV-2 spike: evidence that D614G increases infectivity of the COVID-19 virus, Cell 182 (2020) 812–827, https://doi.org/10.1016/j.cell.2020.06.043, e19.
[9] T.-J. Yang, P.-Y. Yu, Y.-C. Chang, K.-H. Liang, H.-C. Tso, M.-R. Ho, et al., Effect of SARS-CoV-2 B.1.1.7 mutations on spike protein structure and function, Nat. Struct. Mol. Biol. 28 (2021) 731–739, https://doi.org/10.1038/s41594-021-00652-z.
[10] E. Dolgin, Omicron thwarts some of the world's most-used COVID vaccines, Nature 601 (7893) (2022), 311-311, https://www.nature.com/articles/d41586-022-00079-6. (Accessed 26 January 2022).
[11] A. Nag, S. Paul, R. Banerjee, R. Kundu, In silico study of some selective phytochemicals against a hypothetical SARS-CoV-2 spike RBD using molecular docking tools, Comput. Biol. Med. 137 (2021), 104818, https://doi.org/10.1016/j.compbiomed.2021.104818.
[12] M.K. Gupta, S. Vemula, R. Donde, G. Gouda, L. Behera, R. Vadde, In-silico approaches to detect inhibitors of the human severe acute respiratory syndrome coronavirus envelope protein ion channel, J. Biomol. Struct. Dyn. 39 (2021) 2617–2627, https://doi.org/10.1080/07391102.2020.1751300.
[13] Y.H. Li, X.X. Li, J.J. Hong, Y.X. Wang, J.B. Fu, H. Yang, et al., Clinical trials, progression-speed differentiating features and swiftness rule of the innovative targets of first-in-class drugs, Briefings Bioinf. 21 (2019) 649–662, https://doi.org/10.1093/bib/bby130.
[14] H. Yang, C. Qin, Y.H. Li, L. Tao, J. Zhou, C.Y. Yu, et al., Therapeutic target database update 2016: enriched resource for bench to clinical drug target and targeted pathway information, Nucleic Acids Res. 44 (2016) D1069–D1074, https://doi.org/10.1093/nar/gkv1230.
[15] F. Zhu, Z. Shi, C. Qin, L. Tao, X. Liu, F. Xu, et al., Therapeutic target database update 2012: a resource for facilitating target-oriented drug discovery, Nucleic Acids Res. 40 (2012) D1128–D1136, https://doi.org/10.1093/nar/gkr797.
[16] Q. Du, Y. Qian, W. Xue, Molecular simulation of oncostatin M and receptor (OSM–OSMR) interaction as a potential therapeutic target for inflammatory bowel disease, Front. Mol. Biosci. 7 (2020).
[17] W. Xue, F. Yang, P. Wang, G. Zheng, Y. Chen, X. Yao, et al., What contributes to serotonin–norepinephrine reuptake inhibitors' dual-targeting mechanism? The key role of transmembrane domain 6 in human serotonin and norepinephrine transporters revealed by molecular dynamics simulation, ACS Chem. Neurosci. 9 (2018) 1128–1140, https://doi.org/10.1021/acschemneuro.7b00490.
[18] T. Fu, G. Tu, M. Ping, G. Zheng, F. Yang, J. Yang, et al., Subtype-selective mechanisms of negative allosteric modulators binding to group I metabotropic glutamate receptors, Acta Pharmacol. Sin. 42 (2021) 1354–1367, https://doi.org/10.1038/s41401-020-00541-z.
[19] W. Xue, P. Wang, G. Tu, F. Yang, G. Zheng, X. Li, et al., Computational identification of the binding mechanism of a triple reuptake inhibitor amitifadine for the treatment of major depressive disorder, Phys. Chem. Chem. Phys. 20 (2018) 6606–6616, https://doi.org/10.1039/C7CP07869B.
[20] P. Singh, S.S. Chauhan, S. Pandit, M. Sinha, S. Gupta, A. Gupta, et al., The dual role of phytochemicals on SARS-CoV-2 inhibition by targeting host and viral proteins, J. Tradit., Complementary Altern. Med. 12 (1) (2021) 90–99, https://doi.org/10.1016/j.jtcme.2021.09.001.
[21] J. Yang, X. Lin, N. Xing, Z. Zhang, H. Zhang, H. Wu, et al., Structure-based discovery of novel nonpeptide inhibitors targeting SARS-CoV-2 Mpro, J. Chem. Inf. Model. 61 (8) (2021) 3917–3926, https://doi.org/10.1021/acs.jcim.1c00355, acs.jcim.1c00355.
[22] A. Nag, R. Banerjee, R.R. Chowdhury, C. Krishnapura Venkatesh, Phytochemicals as potential drug candidates for targeting SARS CoV 2 proteins, an in silico study, Virus. Dis. (2021) 1–10, https://doi.org/10.1007/s13337-021-00654-x.
[23] J. Yang, Z. Zhang, F. Yang, H. Zhang, H. Wu, F. Zhu, et al., Computational design and modeling of nanobodies toward SARS-CoV-2 receptor binding domain, Chem. Biol. Drug Des. 98 (2021) 1–18, https://doi.org/10.1111/cbdd.13847.
[24] GISAID - Initiative n.d. https://www.gisaid.org/(accessed January 27, 2022).
[25] A.P. Pandurangan, B. Ochoa-Montaño, D.B. Ascher, T.L. Blundell, SDM: a server for predicting effects of mutations on protein stability, Nucleic Acids Res. 45 (2017) W229–W235, https://doi.org/10.1093/nar/gkx439.
[26] I.T. Desta, K.A. Porter, B. Xia, D. Kozakov, S. Vajda, Performance and its limits in rigid body protein-protein docking, Structure 28 (2020) 1071–1081, https://doi.org/10.1016/j.str.2020.06.006, e3.
[27] G. Ribaudo, P. Coghi, L.J. Yang, J.P.L. Ng, A. Mastinu, M. Memo, et al., Computational and experimental insights on the interaction of artemisinin, dihydroartemisinin and chloroquine with SARS-CoV-2 spike protein receptor-binding domain (RBD), Nat. Prod. Res. (2021) 1–6, https://doi.org/10.1080/14786419.2021.1925894.
[28] S. Choudhary, Y.S. Malik, S. Tomar, Identification of SARS-CoV-2 cell entry inhibitors by drug repurposing using in silico structure-based virtual screening approach, Front. Immunol. 11 (2020).
[29] CS de Magalhães, D.M. Almeida, H.J.C. Barbosa, L.E. Dardenne, A dynamic niching genetic algorithm strategy for docking highly flexible ligands, Inf. Sci. 289 (2014) 206–224, https://doi.org/10.1016/j.ins.2014.08.002. Complete:206–24.
[30] C. Kutzner, S. Páll, M. Fechner, A. Esztermann, B.L. de Groot, H. Grubmüller, More bang for your buck: improved use of GPU nodes for GROMACS 2018, J. Comput. Chem. 40 (2019) 2418–2431, https://doi.org/10.1002/jcc.26011.
[31] A.W. Schüttelkopf, D.M.F. van Aalten, PRODRG: a tool for high-throughput crystallography of protein-ligand complexes, Acta Crystallogr. Sect. D Biol. Crystallogr. 60 (2004) 1355–1363, https://doi.org/10.1107/S0907444904011679.
[32] R. Kumari, R. Kumar, , Open Source Drug Discovery Consortium, A. Lynn, g_mmpbsa-a GROMACS tool for high-throughput MM-PBSA calculations, J. Chem. Inf. Model. 54 (2014) 1951–1962, https://doi.org/10.1021/ci500020m.
[33] S.J.A. Rao, N.P. Shetty, Evolutionary selectivity of amino acid is inspired from the enhanced structural stability and flexibility of the folded protein, Life Sci. 281 (2021), 119774, https://doi.org/10.1016/j.lfs.2021.119774.
[34] F.M. Richards, W.A. Lim, An analysis of packing in the protein folding problem, Q. Rev. Biophys. 26 (1993) 423–498, https://doi.org/10.1017/s0033583500002845.
[35] B.S. DeDecker, R. O'Brien, P.J. Fleming, J.H. Geiger, S.P. Jackson, P.B. Sigler, The crystal structure of a hyperthermophilic archaeal TATA-box binding protein, J. Mol. Biol. 264 (1996) 1072–1084, https://doi.org/10.1006/jmbi.1996.0697.
[36] W.T. Harvey, A.M. Carabelli, B. Jackson, R.K. Gupta, E.C. Thomson, E.M. Harrison, et al., SARS-CoV-2 variants, spike mutations and immune escape, Nat. Rev. Microbiol. 19 (2021) 409–424, https://doi.org/10.1038/s41579-021-00573-0.

[37] Q. Li, J. Nie, J. Wu, L. Zhang, R. Ding, H. Wang, et al., SARS-CoV-2 501Y.V2 variants lack higher infectivity but do have immune escape, Cell 184 (2021) 2362–2371, https://doi.org/10.1016/j.cell.2021.02.042, e9.
[38] Z. Liu, L.A. VanBlargan, L.-M. Bloyet, P.W. Rothlauf, R.E. Chen, S. Stumpf, et al., Identification of SARS-CoV-2 spike mutations that attenuate monoclonal and serum antibody neutralization, Cell Host Microbe 29 (2021) 477–488, https://doi.org/10.1016/j.chom.2021.01.014, e4.
[39] Z. Wang, F. Schmidt, Y. Weisblum, F. Muecksch, C.O. Barnes, S. Finkin, et al., mRNA vaccine-elicited antibodies to SARS-CoV-2 and circulating variants, Nature 592 (2021) 616–622, https://doi.org/10.1038/s41586-021-03324-6.
[40] S.-Y. Ren, W.-B. Wang, R.-D. Gao, A.-M. Zhou, Omicron variant (B.1.1.529) of SARS-CoV-2: mutation, infectivity, transmission, and vaccine resistance, World J Clin Cases 10 (2022) 1–11, https://doi.org/10.12998/wjcc.v10.i1.1.
[41] A.B. Jena, N. Kanungo, V. Nayak, Chainy Gbn, J. Dandapat, Catechin and curcumin interact with S protein of SARS-CoV2 and ACE2 of human cell membrane: insights from computational studies, Sci. Rep. 11 (2021) 2043, https://doi.org/10.1038/s41598-021-81462-7.
[42] D. Marín-Palma, J.H. Tabares-Guevara, M.I. Zapata-Cardona, L. Flórez-Álvarez, L. M. Yepes, M.T. Rugeles, et al., Curcumin inhibits in vitro SARS-CoV-2 infection in Vero E6 cells through multiple antiviral mechanisms, Molecules 26 (2021) 6900, https://doi.org/10.3390/molecules26226900.
[43] P.P. Kushwaha, A.K. Singh, K.S. Prajapati, M. Shuaib, S. Gupta, S. Kumar, Phytochemicals present in Indian ginseng possess potential to inhibit SARS-CoV-2 virulence: a molecular docking and MD simulation study, Microb. Pathog. 157 (2021), 104954, https://doi.org/10.1016/j.micpath.2021.104954.
[44] S. Aliebrahimi, S. Montasser Kouhsari, S.N. Ostad, S.S. Arab, L. Karami, Identification of phytochemicals targeting c-met kinase domain using consensus docking and molecular dynamics simulation studies, Cell Biochem. Biophys. 76 (2018) 135–145, https://doi.org/10.1007/s12013-017-0821-6.